



Title:

Repeatability and Accuracy of Laser Scanning-Based Reverse Engineering for Warped Composite Components

Authors:

Eric J. Martin, emarti58@uwo.ca, Western University, Canada
 O. Remus Tutunea-Fatan, rtutunea@eng.uwo.ca, Western University, Canada
 Ryan Gergely, ryan.gergely@gm.com, General Motors, USA
 David A. Okonski, david.a.okonski@gm.com, General Motors, USA

Keywords:

Laser Scanning, Reverse Engineering, Accuracy, Repeatability, Composite Parts, Warpage

DOI: 10.14733/cadconfP.2020.278-285

Introduction:

Undoubtedly, coordinate measurement machines (CMM) have been the ‘gold standard’ in part inspection for several decades. Nonetheless, owed to the improvements in non-contact data acquisition, laser scanners have begun to replace CMMs in many applications including the restoration of cultural artifacts as well as in medical applications [4],[8]. One of the key advantages of laser scanners over CMM is their ability to scan more complex geometries faster [9] as well as their generic applicability to deformable components. However, the accuracy of laser scanners remains relatively low compared to their contact counterparts [1-3],[5-7]. In the vast majority of these studies, CMM was used as the primary validation tool, a route enabled by the high rigidity of the validation sample, typically made out of steel/metal.

The growing number of composite automotive components that are being incorporated in practically every vehicle in order to meet more and more stringent emission standards has brought up new issues with respect to the assessment of part quality. Among them, the difficulties associated with the fixturing of the workpieces that are characterized by warpage patterns constitutes one of the important challenges to be addressed for these parts. The randomness and magnitude of the warpage pattern obtained in the component produced through a high-volume composite manufacturing technology makes the use of conventional fixtures with less fixed datums very challenging. The geometric constraints imposed by the fixed location of the datums can alter the entire ‘free-state’ warpage pattern and hence yield irrelevant post-fixturing measurements. Along the same lines, the simple placement of the warped workpiece on an inspection table will render the CMM useless since the unstable part is prone to move under the action of the measuring probe.

This study is focused on compression molded composite parts that are characterized by relatively large warpage patterns (up to 3 to 4 mm from the nominal shape) as well as a high degree of part to part variability. In this context, the main objective of this work was the identification of an accurate and repeatable technique capable to determine the “free-state” warpage of these parts. This information is critical for manufacturing processes downstream of the initial compression molding, such is the case of assembly operations.

Main Idea:

The main goal of this study was to assess the accuracy and repeatability of the laser scanning-based reverse engineering (RE) procedure as applied on glass fiber reinforced components produced through compression molding. Since the two test components shown in Fig. 1 - termed as seatback outer (SBO) and seatback inner (SBI) - are to be assembled through ultrasonic welding, the gaps between their interior

and exterior flanges have to be precisely assessed prior to entering the assembly phase of the manufacturing process. Furthermore, a warpage-based output metric was used to determine an optimal set of molding conditions. In this context, the accuracy of the RE and dimensional assessment procedure is of paramount importance since it affects both upstream and downstream decisions along the manufacturing chain.

A Faro EDGE laser line probe (LLP) portable scanning arm (calibrated values: accuracy $\pm 25 \mu\text{m}$, repeatability $25 \mu\text{m}$) was used to acquire part geometry data. To assess the errors accumulated in the RE process, a study on the repeatability and accuracy of the results was performed according to the overall plan depicted in Fig. 2. For reference purposes, the dimensions of the bounding box for both composite components was $540 \times 480 \times 98 \text{ mm}$ with a thickness varying between 2.5 and 3.5 mm.

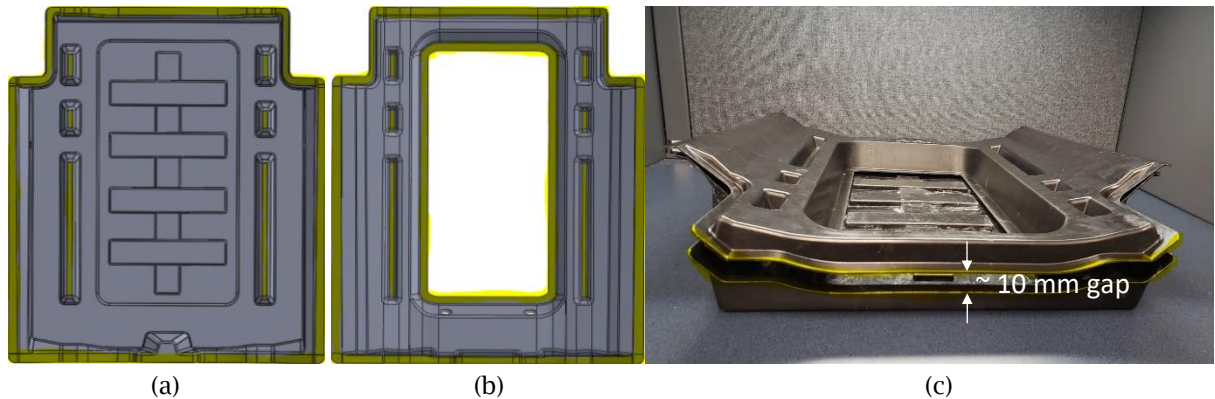


Fig. 1: Sample parts with welding areas highlighted in yellow: (a) seatback outer (SBO), (b) seatback inner (SBI), (c) pre-assembly positioning of SBO (bottom) & SBI (top).

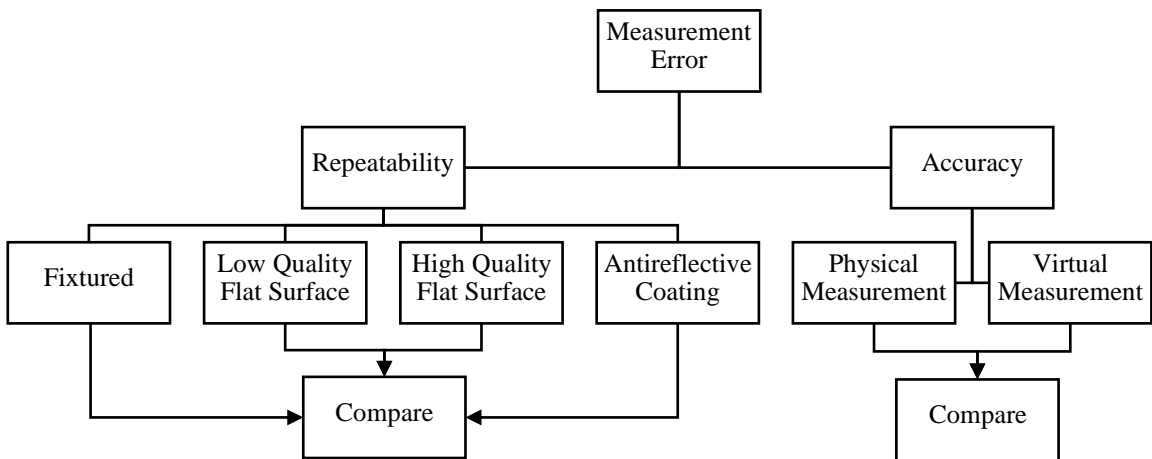


Fig. 2: Error assessment plan.

Repeatability Assessment:

The repeatability of each different RE procedure was evaluated under the same testing conditions and the same data acquisition process. First, clouds of points were acquired by means of a laser scanner. These points were then filtered in the reverse engineering software by means of a user-set standard deviation (0.025 mm) that was determined heuristically. This value provides a threshold at which any points outside of the commonly used range ($\pm 3\sigma$) are being removed on the basis of being outliers.

Evidently, if the value of σ is set too small, then many of the scanned points will be filtered out and the geometry will become difficult to repair due to the numerous defects (i.e., 'holes') introduced in the acquired data. Conversely, if the selected standard deviation is too large, too many outliers will be retained and thereby too much 'noise' will be introduced in the data. According to the trial-and-error tests performed on the analyzed geometries/parts, the chosen value (0.025 mm) - while subjective - appeared to strike a good balance between the completeness and smoothness of the post-filtering data.

After filtering, point cloud data was converted into a triangular mesh. Additional mesh generation controls were used to further improve the quality of the mesh. In this regard, a small rolling ball of 0.5 mm radius was used to further smoothen the geometry and a low reduction rate (2%) was applied in order to improve the flatness of the small near-planar areas that were visible in the data. Larger ball radii could alter the innate fillets/curved regions of the geometry whereas larger decimation rates could inadequately flatten non-planar areas. Same as in the prior step, both parameters were determined through heuristic searches and therefore they are likely only applicable to the geometry analyzed in the present context.

After the completion of the data post-processing phases, two scans of the same part were aligned to each other by employing a conventional best-fit technique. According to the known principles, the best-fit alignment technique aims to minimize all distances between the two geometries to be compared. Owing to the previously mentioned post-processing parameters that were kept consistent for all reconstructed geometries, the best-fit alignment method yielded repeatable results. More specifically, the minor post-processing artifacts that were still present in the geometry did not affect the quality of the relative positioning/alignment between the pair of geometries to be compared. This could also be regarded as a consequence of the global - rather than local - nature of the comparison involved in the best-fitting approaches that essentially allowed elimination of the possible perturbations to be introduced by small data artifacts/defects. The robustness and stability of the best fitting technique was also warranted by the large density of scanned points that were originally acquired: approximately 2M points for SBO and 1M for SBI.

Once the alignment is completed, then differences (termed deviations) between these two scans were measured and exported as tabulated numerical values. Finally, the standard deviation and range of these values were calculated and used to assess the match between pairs of scans. The following sections present several different techniques used to investigate the repeatability.

Fixtured Scanning

To evaluate the effect of fixturing on part warpage, the part was vertically mounted in a fixture whose primary functional was to allow a facile scanning of both A and B sides of the part (Fig. 3a). The fixture was designed with telescopic arms to accommodate scanning of parts of various dimensions and at different laser scanner heights. The resulting standard deviation was ± 0.56 mm. As suggested by Fig.3b, the consistency of the acquired scan data is relatively low with error in both positive and negative directions. The deviations ranged from a maximum of +1.514 mm and a minimum of -1.992 mm.

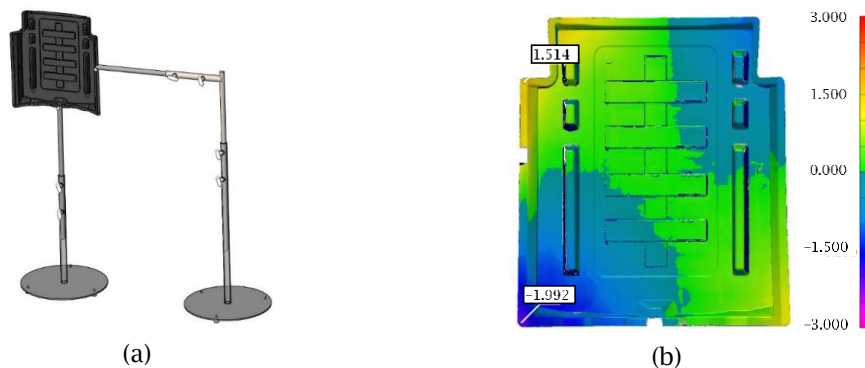


Fig. 3: Repeatability evaluation in part workholding scenario: (a) overview of the fixturing setup, (b) sample deviation map between two replicate scans.

Free-state Scanning on Low Quality Flat Surface

In an effort to improve RE repeatability, alternative scanning and part fixturing schemes were investigated. First, one side of the test part was scanned while resting on the ‘flat’ surface of a typical stainless steel laboratory table. Since no fixturing was used, the part was in its free but warped post-compression molding state. The resulting standard deviation was reduced to ± 0.087 mm. The deviations ranged from a maximum of $+0.216$ mm and a minimum of -0.279 mm (Fig. 4a).

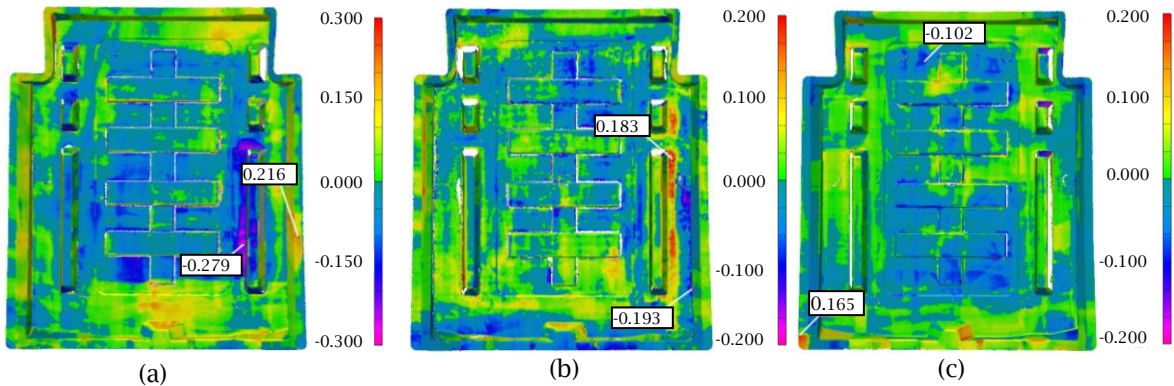


Fig. 4: Sample paired comparisons between replicate scans: (a) unclamped on low quality flat surface, (b) unclamped on high quality surface, (c) scenario (b) covered with antireflective coating.

Free-state Scanning on High Quality Flat Surface

Since both the stability of the table and the flatness of the laboratory table were questionable, the prior laser scanning experiments were repeated on a high quality laboratory table with a granite slab. The resulting standard deviation was further reduced to ± 0.059 mm. The deviations ranged from a maximum of $+0.183$ mm and a minimum of -0.193 mm (Fig. 4b).

Antireflective Coating

To evaluate the possibility of further enhancing the repeatability of the scanning operation, an opaque white powder was applied in order to reduce/eliminate the artifacts introduced by the black and reflective surface of the composite components. After a new set of scans was performed in the free-state on the granite table, the resulting standard deviation of the measured deviations between two replicate scans was again further reduced to ± 0.047 mm. The deviations ranged from a maximum of $+0.165$ mm and a minimum of -0.102 mm (Fig. 4c).

Discussion

A summary of the discrepancies measured between pairs of replicate scans is presented in Tab. 1. Here, StDev is one standard deviation (σ) of the measured deviations between two replicate scans. This data suggests that repeatability is best ensured by coating parts with an antireflective coating and scanning in a free-state while resting on a high quality granite table.

Fixtured	Free-state		
	Low Quality Flat Surface	High Quality Flat Surface	Coated on High Quality Flat Surface
StDev [mm]	StDev [mm]	StDev [mm]	StDev [mm]
0.560	0.087	0.059	0.047

Tab. 1: Summary of repeatability results for different scenarios.

Similarly, the overlays between replicate scans depicted in Fig. 5 suggest that the percentage of points outside of the preset range of the deviation map (± 0.1 mm) - presented in gray color - decreases as the repeatability of the scanning technique increases.

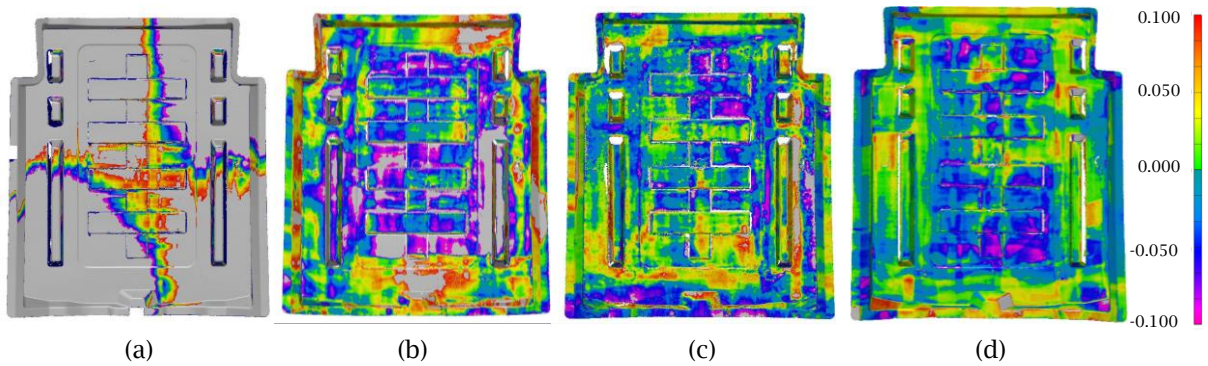


Fig. 5: Direct comparison of replicate scans acquired through different scanning techniques: (a) fixtured, (b) unclamped on low quality flat table, (c) unclamped on high quality flat table, (d) scenario (c) covered with antireflective coating.

Accuracy Study:

Once the repeatability of the process was brought within acceptable limits, the accuracy of the RE process was assessed by means of an RE validation scheme. The physical part was placed with the larger central flat zone in contact with the high quality table and the distance between six different flange points (Fig. 6a) and the flat surface table were measured by means of a touch trigger height measurement gage (accuracy = ± 0.03 mm, repeatability = 0.01 mm). Complementary virtual measurements were determined in a similar manner, but this time by means of the digital model obtained through RE.

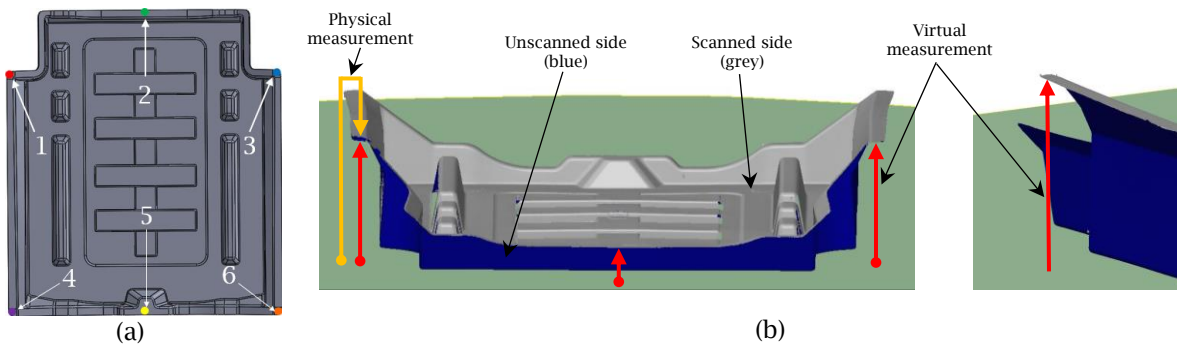


Fig. 6: RE validation protocol for SBO: (a) inspection points, (b) validation distance examples.

Physical Measurements

The distance between the upper/scanned surface of the SBO and flat surface of the table was measured. Triplicate measurements were taken at each of the six locations (Tab. 2). The data collected is characterized by a high level of consistency.

Point Location	Top Left (Point 1)	Top Center (Point 2)	Top Right (Point 3)	Bottom Left (Point 4)	Bottom Center (Point 5)	Bottom Right (Point 6)
Test 1 [mm]	103.39	27.14	103.27	83.25	26.27	83.94
Test 2 [mm]	103.38	27.16	103.33	83.22	26.29	83.89

Test 3 [mm]	103.34	27.17	103.28	83.30	26.28	84.00
Mean [mm]	103.37	27.15	103.29	83.25	26.28	83.94
StDev [mm]	0.026	0.015	0.032	0.040	0.010	0.055

Tab. 2: Distance to the reference surface in the physical setup.

Virtual Measurements

It is important to note that after extensive efforts were made to determine a flat reference plane exclusively by means of the scanned SBO model, this path was eventually abandoned. Two factors were deemed to contribute to this outcome. First, there are numerous RE artifacts in the final SBO mesh that effect the best fitting of the virtual reference plane. Second, the natural position where the part settles is affected by gravity, and not simply the shape of the surface in contact with the table. When attempting to establish a virtual reference plane we found that the actual position and orientation is extremely sensitive to the region of the mesh being included in the planar best fitting. For these reasons, the initial comparisons between virtual and physical measurements were largely discrepant as a consequence of the incorrect positioning of the virtual reference plane. However, the issue of inconsistent virtual reference planes was solved by including a region of the physical table in the original scan of the part and using it to create the virtual reference plane. This enabled consistent and repeatable determinations of the virtual reference plane.

The second observation to be made with respect to the virtual part model is that only its visible side was scanned (Fig. 6a). While specific registration procedures could have been devised in order to align scans of both sides of the part (both acquired while having the part laying down on the table/flat surface), they were deemed outside of the scope of the current study. Mesh vertices located in the area targeted by the physical measurements were selected for distance evaluation purposes. Same as in the physical scenario, triplicate assessments - performed by means of repeated part scans - were used to determine the gaps in the predetermined inspection points. Here also, as in the physical measurements, a high level of consistency was observed in the acquired data (Tab. 3).

Point Location	Top Left (Point 1)	Top Center (Point 2)	Top Right (Point 3)	Bottom Left (Point 4)	Bottom Center (Point 5)	Bottom Right (Point 6)
Scan 1 [mm]	102.975	27.158	103.109	83.315	26.150	83.258
Scan 2 [mm]	103.075	27.183	103.177	83.545	26.202	83.285
Scan 3 [mm]	103.058	27.131	103.263	83.346	26.327	83.320
Mean [mm]	103.036	27.157	103.183	83.402	26.226	83.288
StDev [mm]	0.054	0.026	0.077	0.125	0.091	0.031

Tab. 3: Distance to the reference plane in the virtual setup.

Discussion

Student t-test was used to investigate the level of correlation between physical and virtual inspection metrics. As Tab. 4 suggests, point 1 (top left) and point 6 (bottom right) seem to exhibit statistically different means between physical and virtual measurements ($p < 0.05$). For the remainder of four points, no statistically significant difference can be identified.

Point Location	Top Left (Point 1)	Top Center (Point 2)	Top Right (Point 3)	Bottom Left (Point 4)	Bottom Center (Point 5)	Bottom Right (Point 6)
Physical Mean [mm]	103.370	27.150	103.290	83.250	26.280	83.940
Virtual Mean [mm]	103.036	27.157	103.183	83.402	26.226	83.288
Difference [mm]	0.334	-0.007	0.107	-0.152	0.054	0.652
p-value	0.024	0.972	0.117	0.173	0.415	0.004

Tab. 4: Comparison of physical and virtual accuracy.

The largest contributor to the discrepancy is thought to be movement of the part due to the light contact force induced by the touch-trigger jaw of the height gage. This is evidenced by, the inspection points that are located in the vicinity of the physical contact between the composite part and the reference plane - located close to the projection of top (point 2) and bottom (point 5) center points onto the reference plane - seem to yield measurements that are relatively close between physical and virtual measurement scenarios. This observation underscores the challenges associated with obtaining free-state measurements of warped composite components.

Theoretically, the physical contact points between part and the flat reference plane/surface should be easy to determine. However, part inaccuracies caused by the manufacturing process combined with the artifacts introduced during by the mesh generation process (typically around sharp edges) translate into a difficult task that can only be solved - at least at this time - through visual and tactile inspection of the physical setup. Nonetheless, the biggest drawback of this approach is that it cannot be automated in the digital environment, whereas physical observations tend to be confined to part/surface interface located around the periphery of the part, where a direct line of sight is present. That being said, an overview of all differences that were measured between physical and virtual setup indicates that the largest error found remains under 0.65 mm or 0.8%, assuming the physical measurement as the baseline value.

Conclusions:

The main objective of the current study was to perform an assessment of the repeatability and accuracy associated with the RE process as applied on warped composite components. Unlike most of the prior studies in the field, this work has focused on generating accurate free-state data and demonstrated the effects of poor fixturing.

As such, one of the options that can be employed for scanning of this category of parts consists of the use of a high quality flat surface on which the white-powder coated composite component rests in a free-state. The repeatability and accuracy assessments performed in this setup revealed that: i) paired comparisons of replicate scans would place 98.5% of the scanned points (generally in the range of one-two million per part) within a tolerance of 0.141 mm (3σ) from each other, and ii) high levels of accuracy (within 1% or 0.65 mm) between physical and virtual measurement setups.

Future extensions of this work will aim to compare warped and nominal/unwarped geometries as well as to use the developed techniques towards the assessment of the gap between the two composite components to be joined. This task should be ideally automated in the virtual environment in order to allow - among hundreds of scanned parts - a rapid identification of pairs of SBO and SBI components that are the most suitable for subsequent assembly operations.

Acknowledgements:

The work presented in this study is the result of the collaboration between Western University (London, Canada) and General Motors (Warren, USA). Partial financial support was also provided by Natural Sciences and Engineering Research Council (NSERC) of Canada, Ontario Centers of Excellence (OCE), and General Motors of Canada.

References:

- [1] Ameen, W.; Al-Ahmari, A.; Hammad Mian, S.: Evaluation of handheld scanners for automotive applications, *Applied Sciences*, 8(2), 2018, 217. <https://doi.org/10.3390/app8020217>
- [2] Cuesta, E.; Alvarez, B.; Martinez-Pellitero, S.; Barreiro, J.; Patiño, H.: Metrological evaluation of laser scanner integrated with measuring arm using optical feature-based gauge, *Optics and Lasers in Engineering*, 121(2019), 120-132. <https://doi.org/10.1016/j.optlaseng.2019.04.007>
- [3] Iuliano, L.; Minetola, P.; Salmi, A.: Proposal of an innovative benchmark for comparison of the performance of contactless digitizers, *Measurement Science and Technology*, 21(10), 2010, 105102. <https://www.doi.org/10.1088/0957-0233/21/10/105102>
- [4] Kovacs, L.; Zimmermann, A.; Brockmann, G.; Gühring, M.; Baurecht, H.; Papadopoulos, N.; Schwenzler-Zimmerer, K.; Sader, R.; Biemer, E.; Zeilhofer, H.: Three-dimensional recording of the human face with a 3D laser scanner, *Journal of plastic, reconstructive & aesthetic surgery*, 59(11), 2006, 1193-1202. <https://doi.org/10.1016/j.bjps.2005.10.025>

- [5] Martínez, S.; Cuesta, E.; Barreiro, J.; Alvarez, B.: Methodology for comparison of laser digitizing versus contact systems in dimensional control, *Optics and Lasers in Engineering*, 48(12), 2010, 1238-1246. <https://doi.org/10.1016/j.optlaseng.2010.06.007>
- [6] Michaeli, J. G.; DeGross, M. C.; Roxas, R. C.: Error aggregation in the reengineering process from 3D scanning to printing, *Scanning*, 2017(2017, <http://dx.doi.org/10.1155/2017/1218541>
- [7] Pereira, J. R. M.; de Lima e Silva Penz, I.; da Silva, F. P.: Effects of different coating materials on three-dimensional optical scanning accuracy, *Advances in Mechanical Engineering*, 11(4), 2019, 1687814019842416. <https://doi.org/10.1177/1687814019842416>
- [8] Segreto, T.; Bottillo, A.; Teti, R.; Galantucci, L. M.; Lavecchia, F.; Galantucci, M. B.: Non-contact reverse engineering modeling for additive manufacturing of down scaled cultural artefacts, *Procedia CIRP*, 62(2017, 481-486. <https://doi.org/10.1016/j.procir.2017.03.042>
- [9] Sherman, L. M.: Portable 3D laser scanner slashes molders' inspection time, *Plastics Technology* 61(11), 2017, 72. <https://search.proquest.com/docview/1966055851?accountid=15115&pq-origsite=summon>